Gn blending multiple surfaces in polar coordinates

Kan-Le Shi, Jun-Hai Yong, Jia-Guang Sun, Jean-Claude Paul

G^n blending multiple surfaces in polar coordinates

Kan-Le Shi [a,b,c,d,*], Jun-Hai Yong [a,c,d], Jia-Guang Sun [a,c,d], Jean-Claude Paul [a,c,d,e]

[a] School of Software, Tsinghua University, Beijing 100084, PR China
[b] Department of Computer Science and Technology, Tsinghua University, Beijing 100084, PR China
[c] Key Laboratory for Information System Security, Ministry of Education of China, Beijing 100084, PR China
[d] Tsinghua National Laboratory for Information Science and Technology, Beijing 100084, PR China
[e] INRIA, France

ARTICLE INFO

Article history:
Received 25 May 2009
Accepted 8 November 2009

Keywords:
Multiple surface blending
Polar coordinate
NURBS surface
G^n continuity
N-sided hole filling

ABSTRACT

This paper proposes a method of G^n blending multiple parametric surfaces in polar coordinates. It models the geometric continuity conditions of parametric surfaces in polar coordinates and presents a mechanism of converting a Cartesian parametric surface into its polar coordinate form. The basic idea is first to reparameterize the parametric blendees into the form of polar coordinates. Then they are blended simultaneously by a basis function in the complex domain. To extend its compatibility, we also propose a method of converting polar coordinate blending surface into N NURBS patches. One application of this technique is to fill N-sided holes. Examples are presented to show its feasibility and practicability.

1. Introduction

Blending curves and surfaces is an essential task in geometric modeling [1–3]. It can provide a smooth transition from one curve or surface to another [2,3]. It is also a technique for designing new curves and surfaces [1]. Smoothing corners (called *vertex blending*) and edges (called *edge blending*), and bridging adjacent surfaces are two main applications of blending. Existing blending methods can be classified into two types with regards to the number of blendees: *two-surface blending*, and *multiple surface blending*. The smoothness is measured analogously by parametric continuity C^n or geometric continuity G^n. Engineers and technicians have struggled for decades to achieve higher-order continuity of the blending surface or patches, but so far, a universal, compatible and practical G^n blending model of multiple surfaces is still lacking.

For two-surface blending (e.g., edge blending and the two-surface bridging), both the conic surface and the parametric surface are used as the blending surface. Of existing methods, the classical rolling-ball method was first proposed to get G^1 continuity [4,5]. Then, parametric surfaces were introduced to achieve G^2 [6] and even G^n continuities [1,3,7,8]. As an extension of blending two curves, the two-surface blending methods are mostly based on a one-dimension blending function [1,2,8], which can blend two curves or surfaces once in a specified parametric coordinate.

For more complicated topologies, multiple surface blending techniques were introduced. One of its classical applications is to fill the N-sided hole produced using several intersected surfaces. It is a recurring operation in computer-aided geometric design [9,10] that aims to provide a single surface or surface patches that interpolate the hole's boundary curves satisfying smoothness conditions. The methods of multiple surface blending mainly fall into three categories. The first category splits the blending region into several quadrilateral patches by connecting a center vertex of the hole to the middle point on each boundary curve [11,12]. Piegl [13] used Coons patches to fill N-sided holes with B-spline boundaries and obtained ϵ-G^1 continuity. Yang [10] then extended this method to the NURBS form. Incurring the well-known twist compatibility and tangent compatibility problems, these methods are difficult to be extended to G^2 and higher-order continuities. The second category uses a single patch as the blending surface. Blending functions in both planar polygonal domains [14,15] and nonplanar domains [16,17] were used. Applications of these methods are confined by complicated evaluation, nonstandard representation and the difficulty in satisfying high-order continuity requirements with error control. The third category uses subdivision surfaces. Karčiauskas and Peters [18] introduced a bicubic polar subdivision scheme with C^1 continuity. Then it was extended to C^2 [19,20]. The main target of these methods is to smooth meshes. Continuity between the subdivision surface and the neighboring surfaces is still a challenge in applying their methods to vertex blending. Hwang [9] directly used subdivision surfaces to fill holes with G^1 continuity. Li [21] then achieved C^2 continuity. Mass computation and large memory

* Corresponding author at: School of Software, Tsinghua University, Beijing 100084, PR China.
E-mail address: skl03@mails.tsinghua.edu.cn (K.-L. Shi).

assignment were also introduced by these methods. In summary, the complicated non-NURBS form and low-order smoothness are two key disadvantages of these multiple surface blending methods.

The aim of this paper is to provide a model of blending N parametric surfaces. The basic idea of this method is to blend base surfaces in the circularly symmetric disc-shaped complex domain, which can be represented in polar coordinates. It obtains G^n continuity interiorly, and has G^n-contact with the base surfaces on the boundary. In this method, we first present a definition and continuity conditions of the *polar coordinate parametric surface*. Since it can be represented by existing Cartesian parametric surfaces, the continuity conditions of its NURBS-compatible form are also given. Then the G^n-continuous reparameterization method of converting the blendees in the Cartesian domain into the form of polar coordinates is described. A two-dimension blending formula that blends these polar coordinate parametric surfaces simultaneously is proposed. It is used to fill N-sided holes G^n-continuously without compatibility restrictions of boundaries. To extend its compatibility and practicability, we also propose an approximation method to convert the G^n-continuous blending surface into N NURBS patches.

The organization of this paper is as follows. Section 2 gives the definition and G^n-continuity conditions of the polar coordinate parametric surface. Section 3 extends these conditions to the NURBS-compatible form. Section 4 gives the definition of G^n-continuous reparameterization and proposes a construction method of converting the surfaces in the Cartesian domain into the form of polar coordinates. Section 5 proposes the G^n blending formula of N parametric surfaces. Section 6 presents a simple construction method of converting a polar coordinate blending surface to N approximate NURBS patches. Section 7 introduces the process of filling N-sided holes using this model. Section 8 gives some classical examples. Finally, the paper concludes in Section 9.

2. Continuities of polar coordinate parametric surfaces

Parametric surfaces are mostly defined in the Cartesian domain, which has two orthogonal u- and v-coordinates. Analogously, we can use a complex variable defined in a disc-shaped complex domain as the parameter of a surface. That kind of surface is defined by the following formula (see Fig. 1 (a)):

$$S(z), \quad z \in \mathbb{C} \text{ and } |z| \le 1, \tag{1}$$

where the complex variable z can be represented in polar coordinates (see Fig. 1 (b) and (c)):

$$z = \rho e^{i\theta}, \quad \rho \in [0, 1] \text{ and } \theta \in (-\pi, \pi].$$

In the rest of this paper, $\theta = \arg(z)$ is defined between $-\pi$ and $+\pi$. We call that type of parametric surface the *polar coordinate parametric surface*. It has the following features. First, the parametric domain is circularly symmetric. The surface rotates when a θ-shift is applied. That makes multiple surface blending simpler. Our blending formula proposed in Section 5 uses this feature. Second, there is no corner in the disc-shaped domain ($|z| \le 1$). Algorithms may be simplified by cutting out exceptive handling of corner points. Third, only one special inner point and a circular boundary in parametric domain are considered in continuity conditions instead of four corner points and boundary line segments. Besides, it has natural advantage to represent some conicoids.

Partial derivatives and other differential properties are often defined in a Cartesian system. It is necessary to study the polar coordinate parametric surface in Cartesian coordinates. A mapping is applied to polar coordinates by considering (ρ, θ) (in Eq. (1)) as two orthogonal coordinates in the Cartesian system instead of the length and the angle of the complex number z. To avoid confusion, ρ and θ in the rest of this paper stand for the orthogonal coordinates in the corresponding Cartesian system. The single point $S_0 = S(0, \theta)$ (where θ is arbitrary) in the complex domain is mapped to a line segment $\rho = 0$ in the Cartesian domain. Continuities discussed in this section are mainly about this point and the joint-line (see Fig. 1 (b)). To distinguish the two different meanings of $S(\rho, \theta)$, we write $S^P(\rho, \theta)$ for the polar coordinate parametric surface (with a superscript P) and $S^D(\rho, \theta)$ for the corresponding Cartesian parametric surface (with a superscript D). And we assume that all of the Cartesian parametric surfaces discussed in this paper are *tensor-product surfaces*.

Assume that $S^D(\rho, \theta)$ is an ordinary surface defined in a Cartesian domain (see Fig. 1 (b) and (c)), and that it is G^0-continuous. So the continuity of $S(z)$ only depends on the continuity at the center point and the points on the joint-line. Mathematically, the definition of C^0 continuity at a specified point z_0 can be written in ϵ-δ form as follows.

$$\forall \delta > 0, \exists \varepsilon, \forall z, \text{ if } |z - z_0| < \varepsilon, \text{ we have } |S(z) - S(z_0)| < \delta.$$

Considering the center point and the joint-line, the G^0-continuity conditions of surface $S^P(\rho, \theta)$ are described below.

Condition 1. *Assuming that the regular parametric surface $S^D(\rho, \theta)$ is C^0-continuous, $S^P(\rho, \theta)$ is G^0-continuous, if*

$$\begin{cases} \forall \theta, & \lim\limits_{\rho \to 0^+} S(\rho, \theta) = S(0, \theta) = S_0 \\ \forall \rho, & \lim\limits_{\theta \to -\pi^+} S(\rho, \theta) = S(\rho, +\pi). \end{cases}$$

In Cartesian domains, G^1 continuity requires G^0 continuity of normal vectors as well as the partial derivatives [1,13,22,23]. Analogously to Condition 1, we directly propose the G^1-continuity conditions of polar coordinate parametric surfaces according to the definition of G^1 continuity.

Condition 2. *Assuming that regular parametric surface $S^D(\rho, \theta)$ is C^1-continuous, and that $S^P(\rho, \theta)$ fulfills its G^0-continuity conditions, $S^P(\rho, \theta)$ is G^1-continuous, if the following three equations are all fulfilled:*

$$\left.\frac{\partial S}{\partial \rho}(\rho, \theta)\right|_{\rho=0} \alpha_C(\theta) + \left.\frac{\partial S}{\partial \rho}(\rho, (\theta + \pi)_{\bmod 2\pi})\right|_{\rho=0} \beta_C(\theta) = 0,$$
$$\forall \theta, \exists \alpha_C(\theta) > 0 \text{ and } \beta_C(\theta) > 0, \tag{2}$$

$$\left.\frac{\partial S}{\partial \rho}(\rho, \theta_1)\right|_{\rho=0} \alpha_P(\theta_1) + \left.\frac{\partial S}{\partial \rho}(\rho, \theta_2)\right|_{\rho=0} \beta_P(\theta_2) + \left.\frac{\partial S}{\partial \rho}(\rho, \theta_3)\right|_{\rho=0} \gamma_P(\theta_3) = 0,$$
$$\forall \theta_1 \ne \theta_2 \ne \theta_3 \ne \theta_1, \exists \alpha_P(\theta_1)\beta_P(\theta_2)\gamma_P(\theta_3) \ne 0, \tag{3}$$

and

$$-\left.\frac{\partial S}{\partial \theta}(\rho, \theta)\right|_{\theta \to +\pi} \alpha_L(\rho) + \left.\frac{\partial S}{\partial \theta}(\rho, \theta)\right|_{\theta=-\pi} \beta_L(\rho) + \left.\frac{\partial S}{\partial \rho}(\rho, \theta)\right|_{\theta=-\pi} \gamma_L(\rho) = 0,$$
$$\forall \rho, \exists \alpha_L(\rho) > 0, \beta_L(\rho) > 0 \text{ and } \gamma_L(\rho) \ge 0. \tag{4}$$

Eq. (2) ensures G^1 continuity of an arbitrary isoparametric curve across the center point S_0. Eq. (3) shows that all tangent vectors from the center point are coplanar. Since all Cartesian parametric surfaces are assumed as tensor-product surfaces, Liang's [23] G^1-continuous condition can be applied on the joint-line (see Eq. (4)).

Assuming that there is a specified point on a surface, the plane spanned by a tangent vector and the normal vector is called

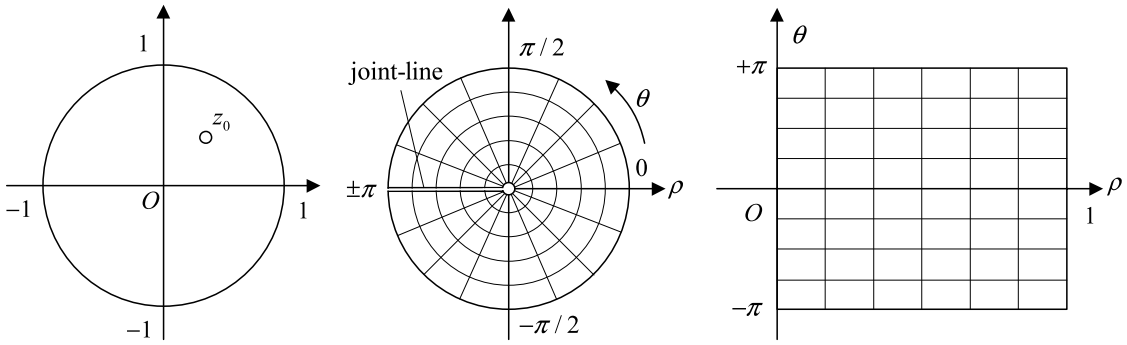

(a) Complex parametric domain. (b) (ρ, θ) represented complex parametric domain. (c) (ρ, θ) rectangular domain.

Fig. 1. Complex domain and its rectangular compatible form.

the *cross-normal plane* of the point. Each intersection curve of the surface and the cross-normal plane has a curvature at that point. According to the definition [23,24], if all curves $S(\rho, \theta)|_{\theta=\theta_0}$ have C^2-contact with the corresponding cross-normal plane, the expression of curvature vector of the center point can be written as

$$k(\theta) = \left(\frac{\partial S}{\partial \rho}(\rho, \theta)\Big|_{\rho=0} \times \frac{\partial^2 S}{\partial \rho^2}(\rho, \theta)\Big|_{\rho=0} \right) \Big/ \left\| \frac{\partial^2 S}{\partial \rho^2}(\rho, \theta)\Big|_{\rho=0} \right\|^3.$$

The conditions of the curvature continuity are as follows.

Condition 3. *Assuming that the regular parametric surface $S^D(\rho, \theta)$ is C^2-continuous, that $S^P(\rho, \theta)$ fulfills its G^1-continuity conditions, and that $S(\rho, \theta)|_{\theta=\theta_0}$ has G^2-contact with its corresponding cross-normal plane, $S^P(\rho, \theta)$ is G^2-continuous at the center point, if the following two conditions are fulfilled:*

$$k(\theta) + k((\theta + \pi)_{\mathrm{mod}\, 2\pi}) = 0, \quad \forall\theta, \tag{5}$$

and

$$k(\theta_1)\alpha_K(\theta_1) + k(\theta_2)\beta_K(\theta_2) + k(\theta_3)\gamma_K(\theta_3) = 0,$$
$$\forall\theta_1 \neq \theta_2 \neq \theta_3 \neq \theta_1, \exists\alpha_K(\theta_1)\beta_K(\theta_2)\gamma_K(\theta_3) \neq 0. \tag{6}$$

The contact condition of $S(\rho, \theta)|_{\theta=\theta_0}$ ensures that the intersection curve of the surface and an arbitrary cross-normal plane can be represented by an isoparametric curve with second-order approximation. The surface curvature in a specified direction is equal to the curvature of one corresponding isoparametric curve. Uniting the G^2-continuity condition of $S^D(\rho, \theta)$, curvature continuity at the center point is proved. Then Eq. (5) ensures that curvatures in opposite directions are compatible. Eq. (6) guarantees that all curvature vectors are coplanar.

The G^2-continuity conditions of adjacent surfaces [23,24] can be directly applied to the joint-line, which can be treated as the common boundary of the left and the right parts of surface $S^D(\rho, \theta)$.

Condition 4. *Assuming that Condition 3 is fulfilled, $S^P(\rho, \theta)$ is G^2-continuous on the joint-line, if*

$$\alpha_L(\rho) D(\rho) = \delta(\rho) D_2(\rho) + \eta(\rho) D_3(\rho), \quad \forall\rho, \exists\delta(\rho), \eta(\rho),$$

where

$$D(\rho) = (\alpha_L(\rho))^2 D_4(\rho) - (\beta_L(\rho))^2 D_5(\rho) - 2\beta_L(\rho)\gamma_L(\rho) D_6(\rho) - (\gamma_L(\rho))^2 D_7(\rho),$$

$$D_2(\rho) = \frac{\partial S}{\partial \theta}(\rho, \theta)\Big|_{\theta=-\pi}, \quad D_3(\rho) = \frac{\partial S}{\partial \rho}(\rho, \theta)\Big|_{\theta=-\pi},$$
$$D_4(\rho) = \frac{\partial^2 S}{\partial \theta^2}(\rho, \theta)\Big|_{\theta\to+\pi}, \quad D_5(\rho) = \frac{\partial^2 S}{\partial \theta^2}(\rho, \theta)\Big|_{\theta=-\pi},$$
$$D_6(\rho) = \frac{\partial^2 S}{\partial \rho \partial \theta}(\rho, \theta)\Big|_{\theta=-\pi}, \quad D_7(\rho) = \frac{\partial^2 S}{\partial \rho^2}(\rho, \theta)\Big|_{\theta=-\pi},$$

and $\alpha_L(\rho)$, $\beta_L(\rho)$ and $\gamma_L(\rho)$ are the same as those defined in Eq. (4).

Conditions 2 and 3 can be extended to G^n for regular polynomial based parametric surfaces. Suppose that $C_{\theta_0}(\tau)$ $(\theta_0 \in (-\pi, +\pi])$ is the natural curve $(\|C'_{\theta_0}(\tau)\| \equiv 1)$ of the isoparametric curve $S(\rho, \theta)|_{\theta=\theta_0}$. And $C^{(n)}{}_{\theta_0}(0)$ is the nth-order derivative vector of $C_{\theta_0}(\tau)$ at the center point $(\tau \to 0)$. We have the following condition.

Condition 5. *Assuming that the regular parametric surface $S^D(\rho, \theta)$ is C^n-continuous, that $S^P(\rho, \theta)$ fulfills its G^{n-1}-continuity conditions, and that $S(\rho, \theta)|_{\theta=\theta_0}$ has G^n-contact with its corresponding cross-normal plane, $S^P(\rho, \theta)$ is G^n-continuous at the center point, if the following two conditions are fulfilled:*

$$C^{(n)}{}_{\theta}(0) + (-1)^{(n+1)} C^{(n)}{}_{(\theta+\pi)_{\mathrm{mod}\, 2\pi}}(0) = 0, \quad \forall\theta,$$

and

$$\begin{cases} C^{(n)}{}_{\theta_1}(0)\alpha(\theta_1) + C^{(n)}{}_{\theta_2}(0)\beta(\theta_2) + C^{(n)}{}_{\theta_3}(0)\gamma(\theta_3) = 0, \\ \quad \forall\theta_1 \neq \theta_2 \neq \theta_3 \neq \theta_1, \exists\alpha(\theta_1)\beta(\theta_2)\gamma(\theta_3) \neq 0, \text{ if } n \text{ is odd} \\ C^{(n)}{}_{\theta} \equiv K, \quad \forall\theta, \text{ if } n \text{ is even}. \end{cases}$$

G^n-continuity conditions of the points on the joint-line are more complicated than Condition 4 [24]. A practical method to ensure the continuity of the joint-line is to let all of the higher-order partial cross-boundary derivatives be equal to zero.

3. Continuities of polar coordinate NURBS surfaces

$S^P(\rho, \theta)$ is called a *polar coordinate NURBS surface* if $S^D(\rho, \theta)$ is in NURBS form. It inherits the continuity features of NURBS surfaces because the transform $z(\rho, \theta) = \rho e^{i\theta}$ is C^n-continuous. And therefore, all of the continuity preconditions about $S^D(\rho, \theta)$ are satisfied if there are no inner multiple knots in the NURBS definition. Conditions in Section 2 can be applied to polar coordinate NURBS surfaces in the following form:

$$S(u, v) = \sum_{i=0}^{n} \sum_{j=0}^{m} N_{i,p}(u) N_{j,q}(v) P^{\omega}_{i,j}, \tag{7}$$

where $N_{i,p}(u)$ and $N_{j,q}(v)$ are B-spline basis functions, and

$$\begin{cases} U = \{\underbrace{0,\ldots,0}_{p+1}, u_{p+1},\ldots,u_{r-p-1}, \underbrace{1,\ldots,1}_{p+1}\}, & r = n+p+1 \\ V = \{\underbrace{0,\ldots,0}_{q+1}, v_{q+1},\ldots,v_{s-q-1}, \underbrace{1,\ldots,1}_{q+1}\}, & s = m+q+1, \end{cases}$$

are the knot vectors of the two dimensions. $P^{\omega}_{i,j} = (X_{i,j}\omega_{i,j}, Y_{i,j}\omega_{i,j}, Z_{i,j}\omega_{i,j}, \omega_{i,j})^T$ are in *homogeneous coordinates*. $P_{i,j} = \left(X_{i,j}, Y_{i,j}, Z_{i,j}\right)^T$ represent the original points and $A_{i,j} = \left(X_{i,j}\omega_{i,j}, Y_{i,j}\omega_{i,j}, Z_{i,j}\omega_{i,j}\right)^T$ represent the first three elements of $P^{\omega}_{i,j}$. The following linear mapping is used to map (u, v) to (ρ, θ).

$$\theta = \begin{cases} 2\pi u - \pi, & u \in (0, 1] \\ +\pi, & u = 0 \end{cases}$$
$$\rho = v.$$

According to Condition 1, for the polar coordinate NURBS surface, we have

Condition 6. *The polar coordinate NURBS surface (defined by Eq. (7)) is G^0-continuous, if*

$$\begin{cases} P_{i,0} = S_0, & i = 0, 1, \ldots, n \\ P_{0,j} = P_{n,j}, & j = 0, 1, \ldots, m. \end{cases}$$

If the NURBS surface $S^D(\rho, \theta)$ is G^1-continuous interiorly (for most instances, this is fulfilled), we only need to consider Condition 2 on the boundary. For the uniform B-spline surface with n control points in the u-direction ($n = 2\eta, \eta \in \mathbb{Z}^+$), the G^1-continuity conditions can be expressed in the following compact form:

$$\begin{cases} \dfrac{P_{i,1} - P_{i,0}}{\left\|P_{i,1} - P_{i,0}\right\|} \cdot \dfrac{P_{i+\eta,1} - P_{i+\eta,0}}{\left\|P_{i+\eta,1} - P_{i+\eta,0}\right\|} + 1 = 0, \quad i = 0, 1, \ldots, n \\ \left(P_{i,1} - P_{i,0}\right) \cdot N = 0, \quad \exists N, i = 0, 1, \ldots, n, \end{cases}$$

where N is the normal vector of the center point. In numerical calculus, we often choose

$$N = \frac{1}{n}\sum_{i=0}^{n-1}\left(P_{i+1,1} - P_{i+1,0}\right) \times \left(P_{i,1} - P_{i,0}\right).$$

We denote that the joint-line is $\left(C(\rho) = S(\rho, \theta)|_{\theta \to +\pi}\right)$, its derivative curve is $\left(D_{\rho}(\rho) = \frac{\partial S}{\partial \theta}(\rho, \theta)\big|_{\theta \to +\pi}\right)$, and their two cross-boundary derivatives are $\left(D_{\theta^+}(\rho) = \frac{\partial S}{\partial \theta}(\rho, \theta)\big|_{\theta = -\pi}\right)$ and $\left(D_{\theta^-}(\rho) = -\frac{\partial S}{\partial \theta}(\rho, \theta)\big|_{\theta \to +\pi}\right)$. They are all represented in NURBS with the same degree and knots (degree elevation and knot refinement may be applied). The following is a sufficient condition of G^1 continuity on the joint-line.

$$\alpha_l D_{\rho}[i] + \beta_l D_{\theta^+}[i] + \gamma_l D_{\theta^-}[i] = 0, \quad \forall i, \exists \alpha_l^2 + \beta_l^2 + \gamma_l^2 \neq 0,$$

where $D_{u+}[i]$ and $D_{u-}[i]$ are the control points of the two derivative curves (square brackets always denote the control points of NURBS curves or surfaces in this paper).

For G^2 and higher-order continuity, an analogous approach can be used. The center point and the points on the joint-line are considered. Furthermore, it is not wise to expand the high-order derivatives into NURBS form because of the explosive increment of complexity. Instead, we had better let the high-order derivatives be equal to a constant value (e.g., zero) in order to reduce the complexity. This is efficient and practical, especially for G^n-continuous surface construction.

4. G^n-continuous reparameterization from the Cartesian domain to the complex domain

G^n continuity is an intrinsic geometric property of curves and surfaces. Suppose that a surface is C^n in parameterization A, and that parameterization B is constructed by applying an operator σ to A. We call the reparameterization from A to B C^n-continuous if the surface is also C^n-continuous in B. This means that, after applying σ, parametric continuity is preserved. The shapes of the domains also effect the continuity of the resulting surface. In order to keep the original continuity, considering σ as a mapping from one Euclidian space α to another Euclidian space β, it is obvious that C^n continuity of σ is a sufficient condition.

Since geometric features and continuity properties should be preserved, reparameterization between two domains of different shapes is more complicated (e.g., a reparameterization from Cartesian coordinates to polar coordinates, which is discussed in Sections 2 and 3). To distinguish these kinds of reparameterization from the ordinary C^n-continuous ones, we call them *G^n-continuous reparameterizations*.

In this section, a simple G^n-continuous reparameterization between the polar coordinate disc-shaped domain and the Cartesian rectangular domain is proposed. It maps surfaces defined in the Cartesian rectangular domain, such as a tensor-product surface, to polar coordinate parametric domain without loss of continuity.

4.1. Definitions and theorems

In this paper, a reparameterization is defined by mapping

$$\sigma : C \to D,$$

where C is the original parametric domain and D is the target parametric domain. On the other hand, σ also can be treated as a surface. C is its parametric domain and its image is in D. We first propose a sufficient G^n-continuity condition of a reparameterization.

Condition 7. *Parameterization σ is G^n-continuous if* (1) *σ and σ^{-1} are both C^n-continuous differentiable functions, and* (2) *the surface σ is G^n-continuous.*

Condition 7 can be roughly proved as follows. Assume that $S(x)$ is a surface, where x is defined in an arbitrary domain. Apply σ^{-1}, which satisfies Condition 7, to x, and we have $S(x) = S(\sigma(y))$. Considering S as a mathematical function and that $S(x)$ is C^n-continuous, the composite function $S(\sigma(y))$ is C^n-continuous. Geometric continuity of surface σ ensures the continuity at special points.

Then, assume that Ψ maps the polar coordinate disc-shaped domain $\mathbb{O} = \{z \,||z| \leq 1, z \in \mathbb{C}\}$ to the Cartesian rectangle domain $\mathbb{D} = \{(u, v)\,|u, v \in [0, 1]\}$. We have the following necessary condition for constructing a G^n-continuous reparameterization according to Condition 7.

Condition 8. *If Ψ is a G^n-continuous reparameterization, the function $\Psi(z)$, which maps the complex domain $\mathbb{O}$ to the Cartesian domain $\mathbb{D}$, is differentiable and C^n-continuous.*

We write $z = (\rho, \theta)$ or $z = \rho e^{i\theta}$. Uniting the continuity conditions introduced in Sections 2 and 3, we have

Condition 9. *If Ψ is a G^n-continuous reparameterization, Curve $\Psi(\rho, \theta_0) \cup \Psi(\rho, (\theta_0 + \pi)_{\mathrm{mod}\,2\pi})$ (arbitrary fixed θ) is G^n-continuous. Curve $\Psi(\rho_0, \theta)$ (ρ_0 is fixed) is closed and G^n-continuous.*

4.2. Domain mapping function Ψ

Before constructing reparameterization Ψ, we first introduce a one-dimension blending function proposed by Hartmann [1].

$$b_{n,\mu}(t) = \frac{\mu(1-t)^{n+1}}{\mu(1-t)^{n+1} + (1-\mu)t^{n+1}},$$
$$t \in [0, 1], \mu \in (0, 1) \text{ and } n \in N_0. \tag{8}$$

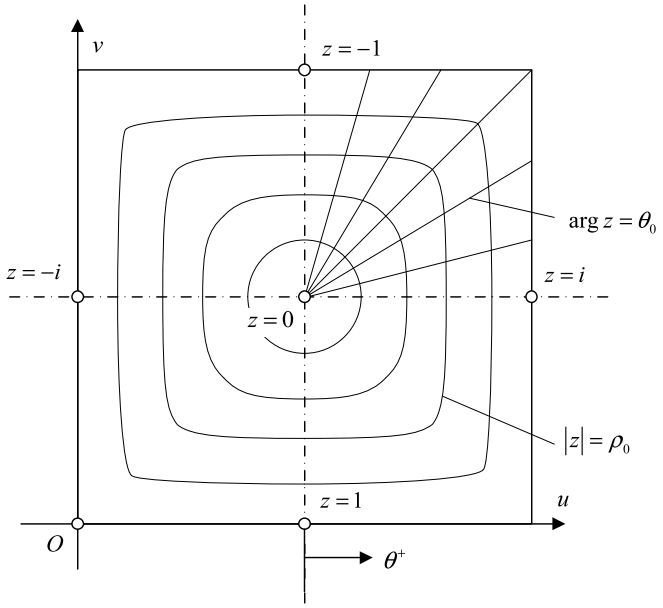

Fig. 2. Isoparametric curves of Ψ mapping.

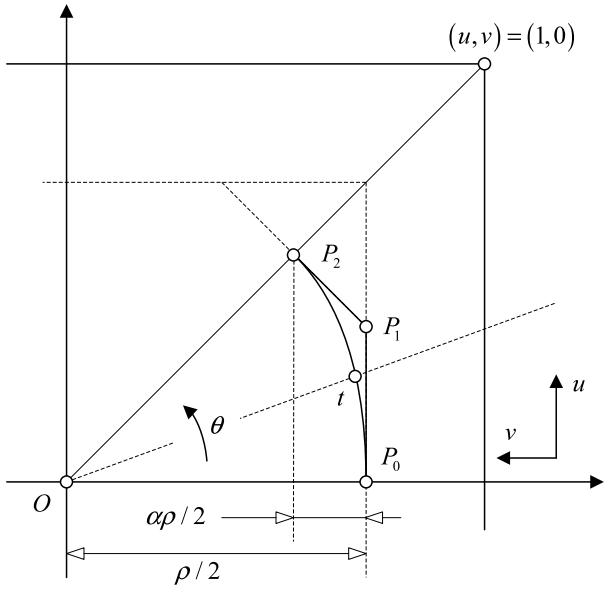

Fig. 3. G^1-Υ construction.

He proved that $b_{n,\mu}$ is C^n-continuous, and that it fulfills the following conditions.

$$b_{n,\mu}(0) = 1, \qquad b_{n,\mu}(1) = 0, \qquad b^{(k)}_{n,\mu}(0) = b^{(k)}_{n,\mu}(1) = 0, \quad k = 1, \ldots, n.$$

Additionally, if n is considered as a variable in $\mathbb{R}^+$, with μ fixed, the two-dimension function $b_\mu(n, t)$ is also continuous in arbitrary order. This property is used in the rest of the paper.

Fulfilling Conditions 8 and 9, a vector mapping Ψ from $\mathbb{O}$ to $\mathbb{D}$ is presented (see Fig. 2). It has two basic properties. First, the center point $z = 0$ is mapped to $(1/2, 1/2) \in \mathbb{D}$. Second, the boundary of $\mathbb{O}$ is mapped to the boundary of $\mathbb{D}$. Define

$$\Psi(\rho, \theta) = \Phi(\rho, \theta)\, b_{n,1/2}(\rho) + \Upsilon(\rho, \theta)\left(1 - b_{n,1/2}(\rho)\right),$$

where

$$\Phi(\rho, \theta) = \begin{pmatrix} u(\rho, \theta) \\ v(\rho, \theta) \end{pmatrix} = \begin{pmatrix} \frac{1}{2}\rho \sin\theta + \frac{1}{2} \\ -\frac{1}{2}\rho \cos\theta + \frac{1}{2} \end{pmatrix}. \tag{9}$$

$\Psi(\rho, \theta)$ is an ordinary blending curve/function of Blend A [2] in the ρ-direction, where $b_{n,1/2}(\rho)$ is the basis function. It blends $\Phi(\rho, \theta)$ and $\Upsilon(\rho, \theta)$, having C^n contact with Φ at the center point and with Υ on the boundary.

$\Phi(\rho, \theta)$ is a set of concentric circles as defined in (9). $\Upsilon(\rho, \theta)$ is more complicated. When $\rho = 1$, Υ maps the boundary circle of domain $\mathbb{O}$ to a square, which is the boundary of domain $\mathbb{D}$. Otherwise, Υ maps concentric circles in domain $\mathbb{O}$ to G^n-continuous closed curves in domain $\mathbb{D}$ (see Fig. 2). It can be constructed using eight $(n + 1)$-degree Bézier curves, which are connected with specified continuity order. The curves $\Upsilon(\rho, \theta)|_{\rho=\rho_0}$ fulfill G^n-continuity conditions and approach the square when $|\rho| \to 1$. Fig. 3 shows one possible instance of G^1-Υ curve. It is patched by eight circularly symmetric two-degree Bézier curves, the first of which is defined by three control points P_0, P_1 and P_2, shown in Fig. 3.

A parameter $\alpha \in [0, 1]$ is used to control the shape of the Bézier curves. When $\alpha \to 0$, the curve approaches the boundary of the square. To get a better shape of the composite Ψ, we restrict ourselves to $\alpha \in \left[0, 1 - \sqrt{2}/2\right]$. Consequently, let

$$\alpha = \left(1 - \frac{\sqrt{2}}{2}\right)(1 - \rho). \tag{10}$$

For the first patch, the parametric curve $\Upsilon_{G^1}(t)$ in (u, v)-coordinates is

$$\Upsilon_{G^1}(t) = \sum_{i=0}^{2} \binom{2}{i} t^i (1 - t)^{2-i} P_i, \tag{11}$$

where

$$\begin{cases} P_0 = \left(\frac{1}{2}, \frac{1}{2} - \frac{1}{2}\rho\right)^T \\ P_1 = \left(\frac{1}{2} + \left(\frac{1}{2} - \alpha\right)\rho, \frac{1}{2} - \frac{1}{2}\rho\right)^T \\ P_2 = \left(\frac{1}{2} + \frac{1}{2}(1 - \alpha)\rho, \frac{1}{2} - \frac{1}{2}(1 - \alpha)\rho\right)^T. \end{cases} \tag{12}$$

Let

$$\frac{u - 1/2}{1/2 - v} = \tan\theta, \tag{13}$$

and unite Eqs. (10), (11) and (13). When (ρ, θ) is fixed, α, P_0, P_1 and P_2 can be calculated using (10) and (12). Then (11) can be expanded to the following quadratic equation:

$$\begin{pmatrix} u \\ v \end{pmatrix} = \begin{pmatrix} a_u t^2 + b_u t + c_u \\ a_v t^2 + b_v t + c_v \end{pmatrix}, \tag{14}$$

where all the coefficients are fixed. Uniting (13) and (14), we have the following quadratic equation with only one variable, t.

$$(a_u + a_v \tan\theta)\, t^2 + (b_u - b_v \tan\theta)\, t + \left(c_u - c_v \tan\theta - \frac{1}{2}(\tan\theta + 1)\right) = 0.$$

The geometric meaning of t is the parameter (on the constructed curve Υ) of the intersection point of the curve Υ and a radial from point O (see Fig. 3). The construction method ensures the existence and uniqueness of the intersection point, and the θ-monotone property of the curve. Thus, that two-degree unitary equation has only one solution in $[0, 1]$. Then we can get (u, v) by (14). So

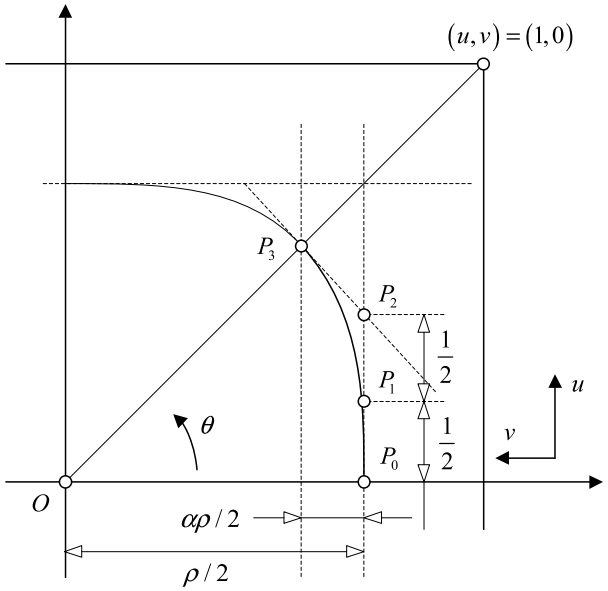

Fig. 4. G^2-Υ construction.

for an arbitrary (ρ, θ), there is only one corresponding (u, v). The mapping expression can be constructed. The constructed function is C^1-continuous in both the θ-direction and the ρ-direction. Furthermore, it can be proved that Ψ fulfills Conditions 7–9. Treating Ψ as a polar coordinate surface, it also fulfills Condition 2. Thus, surface Ψ is G^1-continuous. All the partial derivatives exist. They are C^1-continuous by reason of the analytical form of Ψ. And therefore, Condition 7 is satisfied, and G^1-Ψ is a G^1-continuous reparameterization.

Υ_{G^2} can be constructed analogously. The key challenge is also to construct the G^2-continuous Bézier patches. Fig. 4 shows a construction approach of Υ_{G^2}. According to end-point derivative properties of Bézier curves, all of the eight partial curves are G^2-continuously connected. The definition of the first part of the parametric curve $\Upsilon_{G^2}(t)$ is

$$\Upsilon_{G^2}(t) = \sum_{i=0}^{3} \binom{3}{i} t^i (1-t)^{3-i} P_i,$$

where

$$\begin{cases} P_0 = \left(\frac{1}{2}, \frac{1}{2} - \frac{1}{2}\rho\right)^T \\ P_1 = \left(\frac{1}{2} + \frac{1}{4}(1-2\alpha)\rho, \frac{1}{2} - \frac{1}{2}\rho\right)^T \\ P_2 = \left(\frac{1}{2} + \frac{1}{2}(1-2\alpha)\rho, \frac{1}{2} - \frac{1}{2}\rho\right) \\ P_3 = \left(\frac{1}{2} + \frac{1}{2}(1-\alpha)\rho, \frac{1}{2} - \frac{1}{2}(1-\alpha)\rho\right)^T. \end{cases}$$

After solving a three-degree unitary polynomial equation, the final expressions of $u(\rho, \theta)$ and $v(\rho, \theta)$ can be derived. We can also prove the continuity of the generated reparameterization analogously to the G^1 one.

Summarizing the Υ_{G^1} and Υ_{G^2} construction processes above, the main steps are

1. Construct eight G^n-continuous curve patches.
2. Write the curves in parametric form (such as Bézier or B-spline).
3. Solve the equation concerning parameter t, which is often an n-degree unitary polynomial.
4. Unite all equations and write out the expressions of $u(\rho, \theta)$ and $v(\rho, \theta)$.

When $n > 4$, it is proved that no analytical solution can be found by solving the n-degree polynomial equation. One solution is to use three-degree B-spline curves instead of the high-degree Bézier curves. Or, a closed periodic B-spline curve can be an alternative choice. Theoretically, for arbitrary n, G^n-continuous Υ and the corresponding Ψ can be constructed by these methods.

4.3. θ-$(\pi/4 \to \pi/N)$ continuous mapping

The θ-isoparametric curves of the two-dimension vector function Ψ are nonuniform, symmetrical and straight lines shown in Fig. 2. A θ-nonuniformity adjustment

$$\Theta : [-\pi, +\pi] \to [-\pi, +\pi]$$

is often applied before Ψ mapping (see Fig. 5) in N-surface blending. It is required to map the original θ from $\pi/4$ to π/N with C^n continuity. Θ is considered as both an unitary function $\Theta(\theta)$ and a binary function

$$\Theta(\rho, \theta) = \begin{pmatrix} \Theta_\rho(\rho, \theta) \\ \Theta_\theta(\rho, \theta) \end{pmatrix} = \begin{pmatrix} \rho \\ \Theta(\theta) \end{pmatrix},$$

which has no effect on ρ. We denote $\Psi(\Theta(\rho, \theta)) = (\Psi \circ \Theta)(\rho, \theta)$ if $N \neq 4$. In order to preserve the continuity of the composite function $(\Psi \circ \Theta)$, the following conditions should be satisfied:

$$\Theta\left(\frac{\pi}{N}\right) = \frac{\pi}{4}, \tag{15}$$

and

$$\begin{cases} \Theta(0) = 0 \\ \Theta(-\pi) = -\pi \\ \Theta(+\pi) = +\pi \\ \Theta^{(n)}(-\pi) = \Theta^{(n)}(+\pi) \\ \Theta(\theta) + \Theta(-\theta) = 0, \quad \forall\theta \in [-\pi, +\pi]. \end{cases}$$

Furthermore, like Ψ in the previous subsection, Θ also can be treated as a surface. Continuity conditions should be considered, such as

$$\Theta(\theta_1) - \Theta(\theta_2) = \pi, \quad \text{if and only if} \quad \theta_1 - \theta_2 = \pi, \quad \forall\theta_1, \theta_2 \in (-\pi, +\pi]. \tag{16}$$

We can construct Θ using the G^n blending basis function Eq. (8). The following linear blending function is proposed:

$$\Theta_{G^n}(\theta) = \begin{cases} a\pi b_{n,1/2}(\theta/\pi) + (1-a)\theta, & \theta \in [0, +\pi] \\ -a\pi b_{n,1/2}(-\theta/\pi) + (1-a)\theta, & \theta \in [-\pi, 0), \end{cases}$$

where the density parameter $a \in [-1, +1]$. All the conditions are fulfilled except Eq. (15). It can be satisfied by solving the parameter a. And we have

$$a = \frac{\left(1 + 3^{1+n}\right)(N-4)}{3\left(3^n - 1\right)N},$$

where n is the order of continuity and N is the count of blendees used in the following section.

5. Blending multiple surfaces in polar coordinates

A method is proposed in this section, which simultaneously blends multiple surfaces represented in polar coordinates, for arbitrary geometric continuity order n and arbitrary blendee count N. The previous section gives a construction method of G^n-continuous reparameterizations, which map the points in the Cartesian rectangular domain to the polar coordinate disc-shaped domain. Consequently, all the ordinary parametric surfaces, such as a NURBS surface, can be blended after the reparameterization.

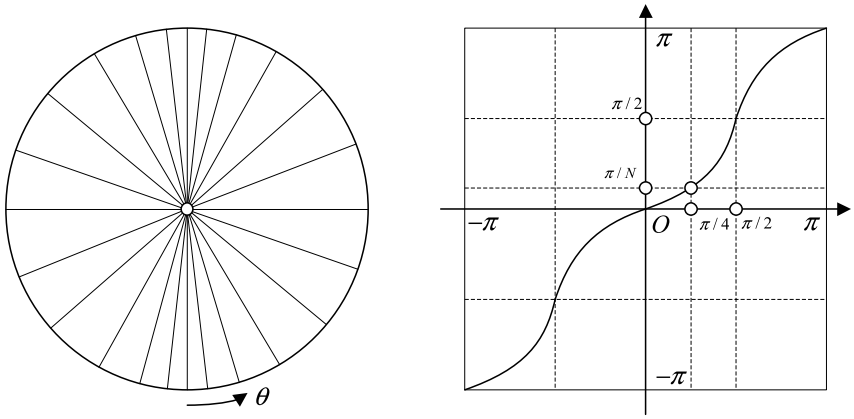

Fig. 5. Sketch map and function curve of θ adjustment.

Blending multiple surfaces is not just an extension of the two-surface parametric blending. It blends spatial surfaces directly using a *two-dimension* weight function, which is more complicated than the one-dimension basis functions since more continuity conditions and boundary restrictions should be considered. The following blending formula of multiple surfaces is defined in the complex domain. It is a linear combination of weighted and rotated original blendees.

$$B(z) = \sum_{i=0}^{N-1} \beta_{i,N}(z)\, S_i\left(z\mathrm{e}^{-\frac{2\pi \mathrm{i}}{N}}\right), \quad z \in \mathbb{O}, \tag{17}$$

where $B(z)$ is the result surface, N is the count of blendees, z is an arbitrary complex number in $\mathbb{O}$, and $\beta_{i,N}$ are weight functions. We assume that the blendees are equivalent (it is sufficient in application). Making use of the circular-symmetry property of domain $\mathbb{O}$, an uniform weight function is introduced:

$$\beta_{i,N}(z) = \beta_N\left(z\mathrm{e}^{-\frac{2\pi \mathrm{i}}{N}}\right).$$

Then, (17) can be translated into the following form.

$$B(z) = \sum_{i=0}^{N-1} \beta_N\left(z\mathrm{e}^{-\frac{2\pi \mathrm{i}}{N}}\right) S_i\left(z\mathrm{e}^{-\frac{2\pi \mathrm{i}}{N}}\right), \quad z \in \mathbb{O}. \tag{18}$$

5.1. Basis function in polar coordinates

This subsection discusses the properties and construction method of the basis function $\beta_N(z)$ in polar coordinates. Shown in Fig. 6, based on the G^0-continuity conditions on the boundary, we have

$$\beta_N(1,\theta) = \begin{cases} 1, & \theta \in \left(-\dfrac{\pi}{N}, +\dfrac{\pi}{N}\right) \\ 1/2, & \theta = \pm\dfrac{\pi}{N} \\ 0, & \theta \in \left(-\pi, -\dfrac{\pi}{N}\right) \cup \left(+\dfrac{\pi}{N}, +\pi\right]. \end{cases}$$

The scalar function β_N is G^n-continuous in domain $\mathbb{O}$. Thus, according to (17), the blending surface is G^n-continuous interiorly (which can be proved using the conditions proposed in Sections 2 and 3) and has G^n-contact with blendees on the boundary, if all the blendees are G^n-continuous interiorly. By way of parenthesis, that function is discontinuous at two points $\mathrm{e}^{\pm\frac{\pi}{N}\mathrm{i}}$, but this does not affect the continuity of the result. Since β_N is also a weight function, the following normalization condition should be fulfilled.

$$\sum_{i=0}^{N-1} \beta_N\left(z\mathrm{e}^{\frac{2\pi \mathrm{i}}{N}}\right) \equiv 1, \quad \forall z \in \mathbb{O}. \tag{19}$$

Satisfying the conditions above, we construct the following G^n-continuous function.

$$\hat{\beta}_N(\rho,\theta) = \left(b_{n/(1-\rho),1/2}(\Theta(\theta)) - \frac{1}{2}\right)\left(1 - b_{n+1,1/2}(\rho)\right) + \frac{1}{2}.$$

$\hat{\beta}_N(\rho,\theta)$ fulfills all the conditions declared in this subsection except the normalization condition (Eq. (19)). Then we construct the following normalized function:

$$\beta_N(z) = \hat{\beta}_N(z) \Big/ \sum_{i=0}^{N-1} \hat{\beta}_N\left(z\mathrm{e}^{-\frac{2\pi \mathrm{i}}{N}}\right),$$

where n is a specified order of continuity, $z = \rho\mathrm{e}^{\mathrm{i}\theta} \in \mathbb{O}$, and S_i are all θ-nonuniformity adjusted by operator Θ. β_N has the following properties.

1. $\beta_N(z) = 1$ if and only if $|z| = 1$ and $\arg(z) \in (-\frac{\pi}{N}, +\frac{\pi}{N})$.
2. $\beta_N(z) = 0$ if and only if $|z| = 1$ and $\arg(z) \in (-\pi, -\frac{\pi}{N}) \cup (+\frac{\pi}{N}, +\pi)$.
3. $\beta_N\left(\mathrm{e}^{\pm\frac{\pi}{N}}\right)$ are the only two discontinuous points, the values of which are set to $1/2$.
4. $\beta_N(z) \in (0, 1)$, where $|z| < 1$.
5. $\beta_N(0) = 1/N$.

5.2. Process of blending multiple surfaces

The generated blending surface is G^n-continuous since all the steps preserve G^n continuity. The steps of blending multiple Cartesian parametric surfaces are as follows.

1. *Adjust the parametric domains*
   The blendees are defined in the Cartesian rectangular domain with two parametric dimensions u and v. The boundaries $S_i(u,v)|_{v=0}$ need to be connected as a ring (see Fig. 7 (a)). The derivative compatibilities are not strictly required. These blendee surfaces may be linear reparameterized to satisfy $u, v \in [0, 1]$. And they should be flipped if the u-direction is not circular anticlockwise or the v-direction is not forward to the center of the N-sided hole. All kinds of parametric surfaces defined on a rectangular Cartesian domain are available in this algorithm.
2. *Reparameterize the blendees from Cartesian coordinates to polar coordinates*
   Use the algorithm proposed in Section 4 to generate a G^n-continuous reparameterization instance. When the blendee count $N \neq 4$, the θ-$(\pi/4 \to \pi/N)$ nonuniformity adjustment Θ is applied. That ensures that each blendee has an equivalent sector of the blending domain (see Fig. 7 (b)).

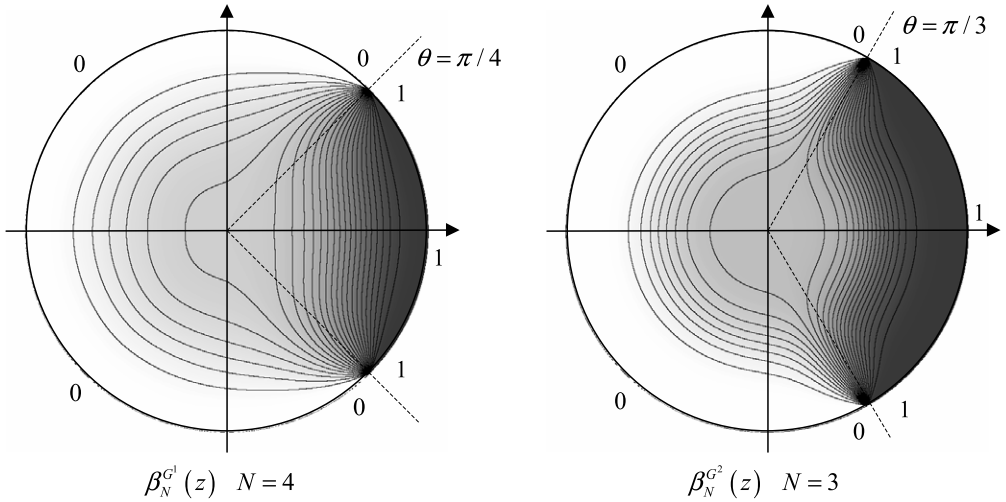

Fig. 6. β functions and their contour maps.

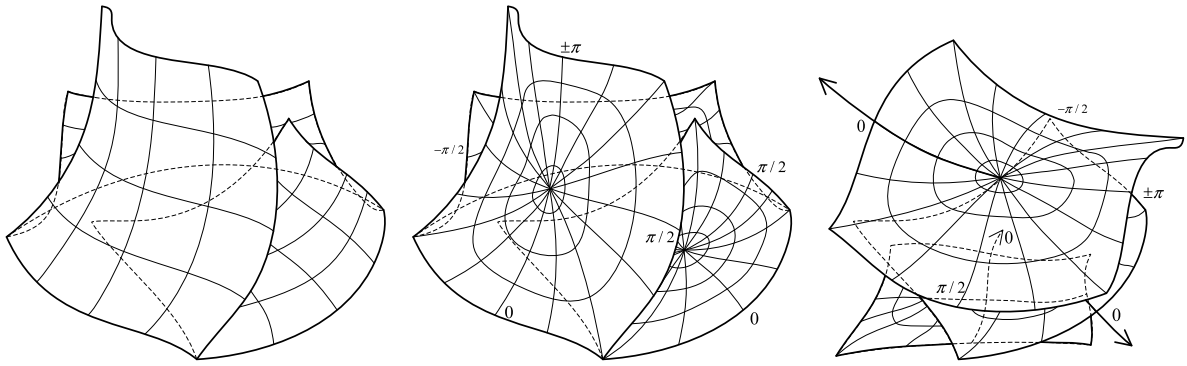

(a) Original blendees. (b) Reparameterized. (c) Blending with phasic offset.

Fig. 7. Blending process.

3. *Blend multiple surfaces using the basis function*
   Each point of the result surface is calculated using (17). The weight function is applied to each blendee and they are summed up with different phasic offsets. Fig. 7 (c) explains the mechanism of this.

The first and the second steps are preprocessed and the results can be stored in a data structure. Calculation of each point is only required while rendering. It is an efficient linear combination of N points of original blendees. The blending surface precisely fulfills all continuity conditions. Furthermore, a more efficient and compatible approach in application, especially in existing CAD/CAM systems, is to convert the blending surface into NURBS patches. The approximation algorithm is discussed in the next section.

This blending technique has the following distinct advantages:

1. G^n-continuity conditions are fulfilled without complicated iteration or equation solving.
2. The algorithm is simple; the main part of it is only a linear combination.
3. There is no need to update or reconstruct the entire surface if the blendees are modified. Weight pre-calculation of each point (which is often the vertex after triangulation) can be applied.
4. Multiple surfaces are blended simultaneously.
5. This method supports incompatible conditions of the boundary (see Fig. 15).

5.3. Properties of the blending surface

This subsection gives the properties of the blending surface. By default, S_i is defined in the Cartesian domain and B is defined in the polar coordinate domain. We first present the formulae concerning the derivatives of the center point. The zeroth-order derivative (the position) of the center point is the arithmetical average of all center points of the blendees in their parametric space:

$$B(0,\theta) = \frac{1}{N}\sum_{i=0}^{N-1} S_i\left(\frac{1}{2},\frac{1}{2}\right), \quad \forall\theta. \tag{20}$$

The first-order derivatives of the center points are the arithmetical average of the corresponding derivatives of the center points on each blendee.

$$\left.\frac{\partial B(\rho,\theta)}{\partial\rho}\right|_{\rho=0} = \frac{1}{N}\sum_{i=0}^{N-1}\left(\left.\frac{\partial S_i}{\partial u}\right|_{\substack{u=1/2\\v=1/2}}\sin\delta - \left.\frac{\partial S_i}{\partial v}\right|_{\substack{u=1/2\\v=1/2}}\cos\delta\right), \tag{21}$$

where

$$\delta = \Theta\left(\theta - \frac{2\pi\mathrm{i}}{N}\right)_{\mathrm{mod}\,2\pi}.$$

Analogously, we have the formula for the second-order derivatives.

$$\left.\frac{\partial^2 B(\rho,\theta)}{\partial\rho^2}\right|_{\rho=0} = \frac{1}{N}\sum_{i=0}^{N-1}\left(\sin^2\delta\left.\frac{\partial^2 S_i}{\partial u^2}\right|_{\substack{u=1/2\\v=1/2}} - \sin 2\delta\left.\frac{\partial^2 S_i}{\partial u\partial v}\right|_{\substack{u=1/2\\v=1/2}} + \cos^2\delta\left.\frac{\partial^2 S_i}{\partial v^2}\right|_{\substack{u=1/2\\v=1/2}}\right). \tag{22}$$

Since β_N is flat and smooth at the center point,

$$\left.\frac{\partial^r \beta_N}{\partial\rho^r}\right|_{\rho=0} = 0, \quad r = 1,2,\ldots,n,$$

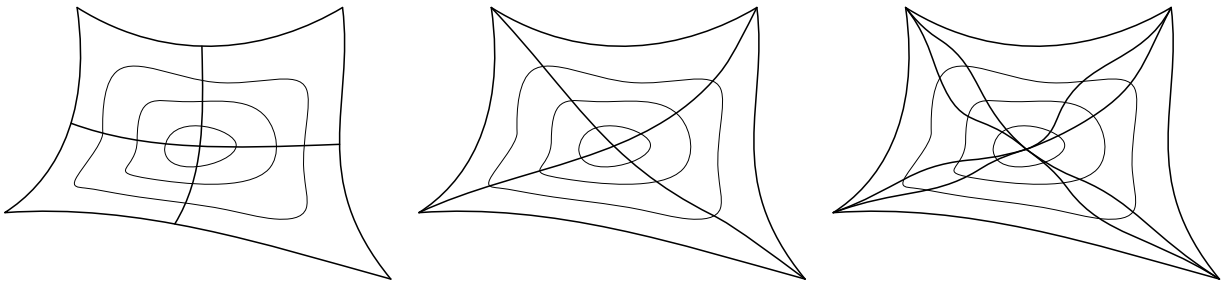

(a) Piegl's quadrilateral patches. (b) Triangular patches. (c) Hybrid patches.

Fig. 8. Approximation NURBS patches.

for high-order derivatives, we have

$$\left.\frac{\partial^n B(\rho,\theta)}{\partial\rho^n}\right|_{\rho=0} = \frac{1}{N}\sum_{i=0}^{N-1}\sum_{j=0}^{n}\binom{n}{j}(-1)^{n-j}\sin^j\delta\cos^{n-j}\delta \times \left.\frac{\partial^n S_i}{\partial u^j\partial v^{n-j}}\right|_{\substack{u=1/2\\v=1/2}}.$$

The formulae above imply that each blendee is equivalent at the center point.

Derivatives of a specified point on the boundary only depend on the corresponding blendee. The zeroth-order derivative (the position) is

$$B(1,\theta)|_{\theta\in\left(\left(-\frac{\pi}{N}+\frac{2\pi i}{N}\right)_{\mathrm{mod}\,2\pi},\left(+\frac{\pi}{N}+\frac{2\pi i}{N}\right)_{\mathrm{mod}\,2\pi}\right)} = S_i\left(\frac{1}{2}+\frac{1}{2}\tan(\Theta(\theta)),0\right).$$

And the first-order derivatives are

$$\left.\frac{\partial B(\rho,\theta)}{\partial\rho}\right|_{\rho=1} = \left.\frac{\partial S_i}{\partial u}\right|_{\substack{u=\frac{1}{2}+\frac{1}{2}\tan(\Theta(\theta))\\v=0}}\frac{\partial u}{\partial\rho} + \left.\frac{\partial S_i}{\partial v}\right|_{\substack{u=\frac{1}{2}+\frac{1}{2}\tan(\Theta(\theta))\\v=0}}\frac{\partial v}{\partial\rho}, \tag{23}$$

where $\frac{\partial u}{\partial\rho}$ and $\frac{\partial v}{\partial\rho}$ are the partial derivatives of the reparameterization between the polar coordinate domain and the Cartesian domain. We can also give the second-order derivatives:

$$\left.\frac{\partial^2 B(\rho,\theta)}{\partial\rho^2}\right|_{\rho=1} = \left.\frac{\partial^2 S_i}{\partial u^2}\right|_{\substack{u=\frac{1}{2}+\frac{1}{2}\tan(\Theta(\theta))\\v=0}}\left(\frac{\partial u}{\partial\rho}\right)^2 + 2\left.\frac{\partial^2 S_i}{\partial u\partial v}\right|_{\substack{u=\frac{1}{2}+\frac{1}{2}\tan(\Theta(\theta))\\v=0}}\frac{\partial u}{\partial\rho}\frac{\partial v}{\partial\rho} + \left.\frac{\partial^2 S_i}{\partial v^2}\right|_{\substack{u=\frac{1}{2}+\frac{1}{2}\tan(\Theta(\theta))\\v=0}}\left(\frac{\partial v}{\partial\rho}\right)^2. \tag{24}$$

Analogously, we have

$$\left.\frac{\partial^n B(\rho,\theta)}{\partial\rho^n}\right|_{\rho=1} = \sum_{i=0}^{n}\binom{n}{i}\left.\frac{\partial^n S_i}{\partial u^i\partial v^{n-i}}\right|_{\substack{u=\frac{1}{2}+\frac{1}{2}\tan(\Theta(\theta))\\v=0}} \times\left(\frac{\partial u}{\partial\rho}\right)^i\left(\frac{\partial v}{\partial\rho}\right)^{n-i}.$$

$$\left.\frac{\partial^r\beta_N}{\partial\rho^r}\right|_{\rho=1} = 0,\quad r=1,2,\ldots,n.$$

The formulae above imply that β_N is flat and smooth on the boundary.

The singular corner points are set to the arithmetical average of the two corresponding corner points (which are always the same if the specified blendees fulfill the compatibility conditions) of the two neighboring blendees.

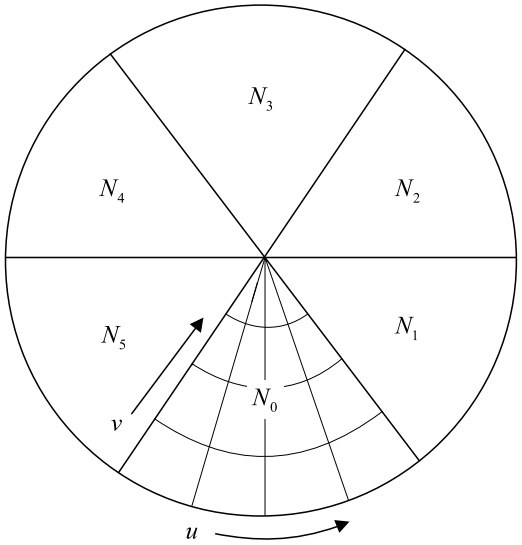

Fig. 9. Parametric symmetrical partition.

6. NURBS approximation

NURBS has already become the de facto industrial standard in existing CAD/CAM systems [10,13,25]. It is required to convert the blending surface discussed in the previous sections into NURBS patches for data exchange and further processing. Section 2 declares that any polar coordinate surface can be represented in Cartesian coordinates. Theoretically, only one NURBS surface is sufficient to represent a polar coordinate blending surface. Further analysis shows that the knot multiplicity in the corner of the approximate NURBS surface may be large enough to split the surface into N NURBS patches equivalently. Thus, we mainly discuss the N-NURBS patching technique instead of the single-NURBS approximation.

Fig. 8 shows three familiar types of patching. Piegl [13] proposed an approach of N quadrilateral patches that incurs compatibility problems for G^1 continuity (see Fig. 8 (a)). This method introduces more compatibility problems for higher-order geometric continuity. To handle these problems, the corners can be split into two (see Fig. 8 (b)) or three (see Fig. 8 (c)) patches. This makes the approximation simpler and more practical. The triangular patch introduces a regressive point (which is the center point of the blending surface). The continuity conditions of this point are discussed in Sections 2 and 3. The following subsections give a construction method to generate N approximate triangular NURBS patches having ϵ-G^1 and ϵ-G^2 contact with the original boundary.

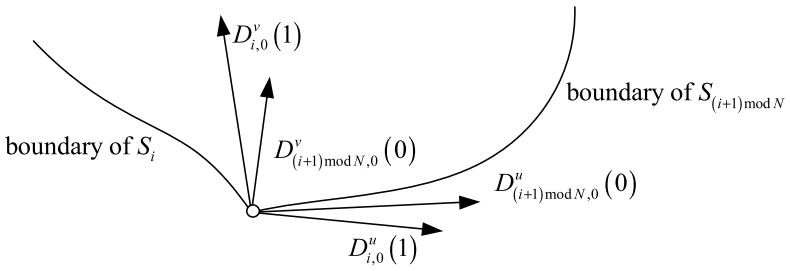

Fig. 10. Incompatible tangent vectors in the corner.

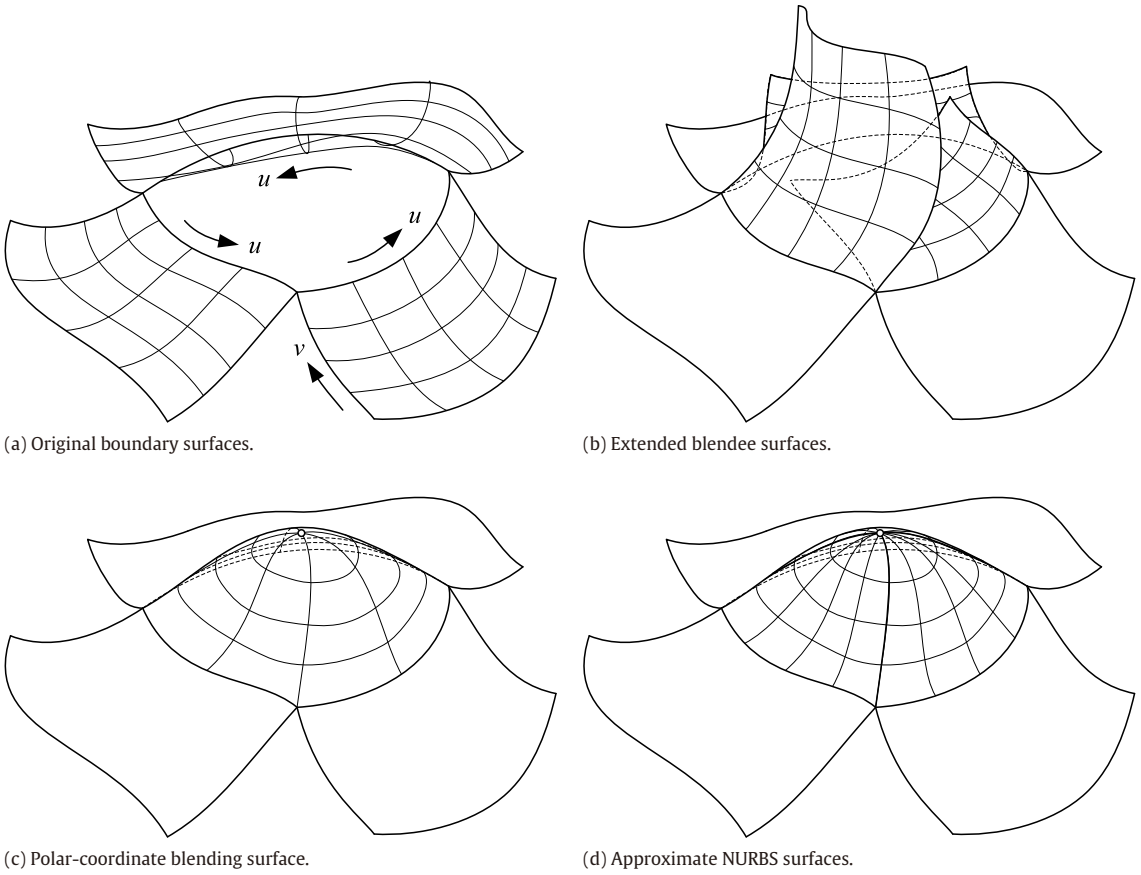

(a) Original boundary surfaces.

(b) Extended blendee surfaces.

(c) Polar-coordinate blending surface.

(d) Approximate NURBS surfaces.

Fig. 11. Process of filling N-sided holes.

6.1. G^1-continuous NURBS approximation

The blending surface is split into N NURBS patches N_i equally in the θ-direction in polar coordinates (see Figs. 8 (b) and 9). Assume that the u-direction of N_i is anticlockwise and that the v-direction is pointing to the center of the blending region (see Fig. 9). The blendees S_i are all converted to available NURBS form in the first step of multiple surface blending. Having G^1-contact with the original boundary, each N_i is constructed following the instructions below.

1. Compute the NURBS form of $D^v_{i,0}(u) = \frac{\partial S_i}{\partial v}(u, v)\Big|_{v=0}$, which is called the *cross-boundary derivative curve*. In the worst case, the degree of $D^v_{i,0}(u)$ is $2p$, where p is the degree of $C_{i,0} = S_i(u, v)|_{v=0}$.
2. Compute the NURBS form of $D^u_{i,0}(u) = \frac{\partial S_i}{\partial u}(u, v)\Big|_{v=0}$. In the worst case, the degree of $D^u_{i,0}(u)$ is also $2p$.
3. Ensure that $D^u_{i,0}(u)$ and $D^v_{i,0}(u)$ have the same degree and share the same knot vector U. Degree elevation and knot refinement may be applied to them. In the worst case, the degree of them is $2p$.
4. According to (23), compute the r-order Taylor series expansion of $\frac{\partial u}{\partial \rho}$ and $\frac{\partial v}{\partial \rho}$ at 0. Compute the approximate NURBS form of the $\frac{\partial u}{\partial \rho}$ and $\frac{\partial v}{\partial \rho}$ series and then apply NURBS scalar multiplication to $D^u_{i,0}(u)$ and $D^v_{i,0}(u)$ in conformity to the formula. Symbolic operators [26] (NURBS addition and multiplication) are applied. Finally, we can get a $(2p + r)$-degree NURBS cross-boundary derivative curve in the polar coordinate parametric space: $D_{i,0}(u) = \frac{\partial B}{\partial \rho}(\rho, \theta)\Big|_{\rho=1}$. This is the cross-boundary derivative curve of $N_i(u, v)|_{v=0}$.
5. Ensure that $C_{i,0}(u)$ and $D_{i,0}(u)$ have the same degree and share the same knot vector. Degree elevation and knot refinement may be applied.
6. Compute the central tangent vectors. Each control point of $D_{i,1}(u)$ associates with one central tangent vector according to (21) in Section 5.3. Then, use these vectors to generate the control points of the curve $D_{i,1}(u)$ in NURBS form.

7. Construct N_i using a three-degree Bézier:

$$\begin{cases} N_i[j,0] = C_{i,0}[j] \\ N_i[j,1] = C_{i,0}[j] + \dfrac{1}{3}D_{i,0}[j] \\ N_i[j,2] = C_{i,1} + \dfrac{1}{3}D_{i,1}[j] \\ N_i[j,3] = C_{i,1}, \end{cases}$$

where $N_i[j, l]$ are the control points of NURBS surface N_i, and $C_{i,1}$ is the center point of the blending surface (see (20)).

The steps generate a rough patch set. After that, some control points should be adjusted to make the best of achieving ϵ-G^1 continuity (discussed in Section 6.3).

6.2. G^2 and higher-order continuous NURBS approximation

Analogously, the following steps construct G^2-continuous approximate NURBS patches.

1. Do steps 1 to 7 of the previous subsection.
2. Compute the NURBS form of $D^{uu}_{i,0}(u)$, $D^{uv}_{i,0}(u)$ and $D^{vv}_{i,0}(u)$, which are the second-order partial derivatives along the corresponding boundary.
3. According to (24), the three NURBS curves $D^{uu}_{i,0}(u)$, $D^{uv}_{i,0}(u)$ and $D^{vv}_{i,0}(u)$ are composed with weight curves approximated by Taylor series expansion. And the second-order cross-boundary derivative $E_{i,0}(u)$ is constructed.
4. According to (22), the control points of the second-order derivative at the center point are computed. And the second-order central derivative curve $E_{i,1}(u)$ can be constructed.
5. Construct N_i using a five-degree Bézier (or three-degree B-spline):

$$\begin{cases} N_i[j,0] = C_{i,0}[j] \\ N_i[j,1] = C_{i,0}[j] + \dfrac{1}{5}D_{i,0}[j] \\ N_i[j,2] = C_{i,0}[j] + \dfrac{2}{5}D_{i,0}[j] + \dfrac{1}{20}E_{i,0}[j] \\ N_i[j,3] = C_{i,1} + \dfrac{2}{5}D_{i,1}[j] + \dfrac{1}{20}E_{i,1}[j] \\ N_i[j,4] = C_{i,1} + \dfrac{1}{5}D_{i,1}[j] \\ N_i[j,5] = C_{i,1}. \end{cases}$$

Constructing NURBS patches precisely for higher-order approximation is not practical because of the unbearable high degree. A solution is to split or decompose the original blending surfaces into kN partitions in the θ-direction instead of only N patches. An approximate degree-reducing algorithm can be applied after splitting. The degree of the Taylor approximation curve also can be reduced by splitting the boundary curve into several segments if necessary.

6.3. Compatibility and continuity of the shared inner boundaries

The specified boundaries of blendees are often incompatible and discontinuous in practice. G^n-compatibility conditions can be rarely fulfilled in the corner. So the control points near the shared inner boundaries of adjacent approximate surfaces should be adjusted to satisfy the compatibility and continuity conditions.

Two adjacent patches should share a common boundary. The following equation needs to be satisfied.

$$\left.\frac{\partial N_i}{\partial v}(u,v)\right|_{\substack{u=1\\v=0}} = \left.\frac{\partial N_{(i+1)\bmod N}}{\partial v}(u,v)\right|_{\substack{u=0\\v=0}}.$$

So (23) is adjusted to fulfill that equation. Two cases are separately considered (see Fig. 10).

1. $D^u_{i,0}(1)$, $D^v_{i,0}(1)$, $D^u_{(i+1)\bmod N,0}(0)$ and $D^v_{(i+1)\bmod N,0}(0)$ are coplanar.

   For ordinary situations, $D^u_{i,0}(1)$ is parallel to $D^v_{(i+1)\bmod N,0}(0)$, and $D^v_{i,0}(1)$ is parallel to $D^u_{(i+1)\bmod N,0}(0)$. So the four vectors are coplanar. In this case, we only need to set

$$D_{i+1/2} = \frac{1}{2}\left(D_{i,0}(1) + D_{(i+1)\bmod N,0}(0)\right).$$

2. $D^u_{i,0}(1)$, $D^v_{i,0}(1)$, $D^u_{(i+1)\bmod N,0}(0)$ and $D^v_{(i+1)\bmod N,0}(0)$ are NOT coplanar.

   That situation appears only if the specified blendees are not compatible in the corner. An arbitrary tangent vector at the corner point of blendee S_i can be represented as $D^*_{i,0}(1) = \alpha D^u_{i,0}(1) + \beta D^v_{i,0}(1)$ where $\alpha, \beta \in \mathbb{R}$. And analogously $D^*_{(i+1)\bmod N,0}(0) = \gamma D^u_{(i+1)\bmod N,0}(0) + \delta D^v_{(i+1)\bmod N,0}(0)$, where $\gamma, \delta \in \mathbb{R}$. $D_{i,0}(1)$ and $D_{(i+1)\bmod N,0}(0)$ are on two concurrent planes. The aim is to find a vector on both the two planes. Since an arbitrary vector on the intersection line of the two planes satisfies that condition, we can set $D_{i+1/2}$ to the one that has the arithmetical or geometric average length of $D_{i,0}(1)$ and $D_{(i+1)\bmod N,0}(0)$.

Represent $D_{i+1/2} = \alpha D^u_{i,0}(1) + \beta D^v_{i,0}(1)$ and $D_{i+1/2} = \gamma D^u_{(i+1)\bmod N,0}(0) + \delta D^v_{(i+1)\bmod N,0}(0)$, where $\alpha, \beta, \gamma, \delta \in \mathbb{R}$. In the NURBS form of Taylor series of $\frac{\partial u}{\partial \rho}$ and $\frac{\partial v}{\partial \rho}$, set the values of the end-points to α, β, γ and δ. This ensures that the cross-boundary tangent vectors in the corner are equal to $D_{i+1/2}$. If we want to bound the modification locally, knot insertion can be applied [13,25]. Besides, after the adjustment, the two adjacent approximate surfaces are not accurately G^1-continuous on the shared boundary. We can insert knots to the original blendees near the common boundary. Since more knots lead to higher precision of the approximation, the error of continuity between the two adjacent surfaces reduces after the knot insertion.

In order to obtain higher-order continuity on the boundary, a simpler and more practical method is to let all the high-order cross-boundary derivatives be equal to zero. Insert knot Δu to the right surface and $1 - \Delta u$ to the left surface. Move the inserted control points to make the two cross-boundary derivatives both equal to zero. More knots can be inserted for higher-order continuity.

In this section, we have proposed a fast and simple approximation method. Since we use the low-degree Bézier as the base curve in the v-direction, it is not precise enough for some special requirements. The following methods might be the candidates of extraordinary applications of high precision.

1. Divide the original approximate NURBS surface into several patches in both the u-direction and the v-direction.
2. Sample points and interpolate them. A better shape is obtained but the continuity is difficult to be preserved.
3. Use Piegl's quadrilateral patching method, which may cause compatibility problems.

Because of the limitations of the NURBS form, only ϵ-G^n-continuous patches can be generated, especially for the situation that all of the specified blendees are not compatible. There is still a lot of work to be done on approximation.

7. *N*-sided hole filling

Filling N-sided holes is fundamental in CAD/CAM systems. Our blending model evades the complicated derivation of high-order continuities and compatibilities. It can generate a G^n-continuous blending surface having G^n-contact with the blendees (proposed in Sections 4 and 5). The blending surface also can be approximated by N NURBS surfaces (introduced in Section 6). Practically, it

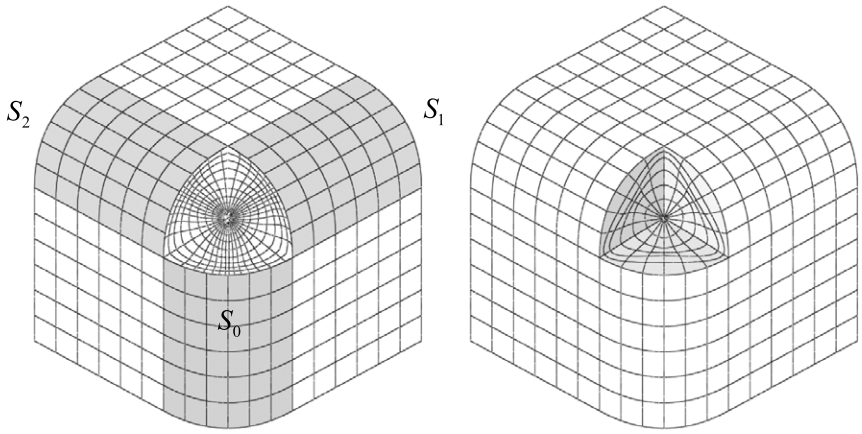

(a) Blending surface. (b) Approximate NURBS surfaces.

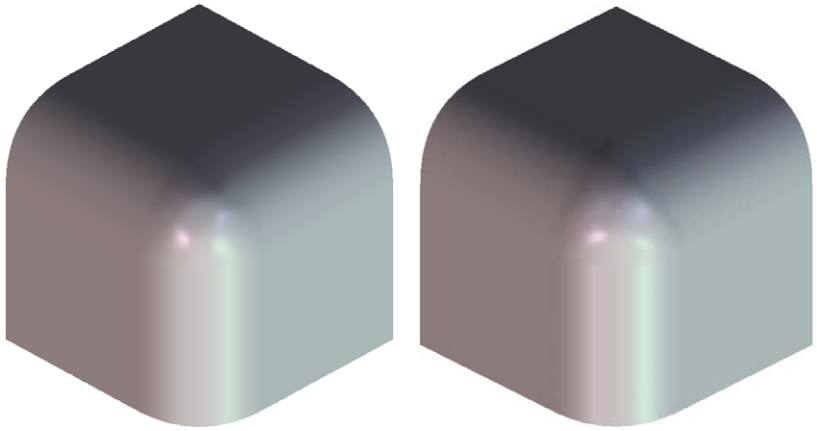

(c) Rendered blending surface. (d) Rendered approximate NURBS patches.

Fig. 12. Example 1: G^2 blending of a three-sided hole.

can be used in filling N-sided holes according to the following steps.

1. *Reparameterize the original surfaces*
   The original surfaces should be defined in Cartesian rectangular domains. Reparameterization may be applied to ensure that (i) $u, v \in [0, 1]$, (ii) the u-directions of boundary surfaces are along the anticlockwise direction, and (iii) the v-directions are pointing to the center of the hole (see Fig. 11 (a)).
2. *Extend the original surfaces to generate blendees*
   Each original surface is extended in the v^+-direction, preserving C^n continuity. The extended surfaces are blendees in the following blending step. Bézier curves may be used in the v-direction. First, the ith-order ($i = 0, 1, \ldots, n$) cross-boundary derivative vectors are computed. For each control point in the u-direction, generate an n-degree Bézier curve that satisfies the boundary derivatives. Then the extended surfaces are constructed using the control points of the Bézier curves (see Fig. 11 (b)).
3. *Apply multiple surface blending*
   Multiple surface blending based on polar coordinate reparameterization is applied to the blendees. The generated blending surface fills the hole with G^n continuity (see Fig. 11 (c)).
4. *NURBS approximation (optional)*
   We can convert the blending surface into NURBS patches. The method introduced in the previous section is applied to generate N or more approximate NURBS patches (see Fig. 11 (d)).

Formula (18) is an all-purpose model of blending multiple surfaces. Once N blendees are decided, the shape of the result is determined. In order to control the shape of the blending surface, it is wise to control the blendees in the second step of extension. Preserving continuity on the common boundary with an original surface, different extension parameters can be applied. That makes the shape control more dynamic and flexible.

Compared with existing methods of filling N-sided hole, this method has several advantages. First, the generated surface is accurately G^n-continuous. Error control in some existing CAD systems (which often use one low-degree trimmed B-spline surface as the blending patch) is needless. In the phase of manufacture, our method can directly generate precise sampling points without interior or boundary errors. The high-order continuity makes the shape better and more propitious to machining. The flat property (see Section 5.3) implies that the blending surface inherits the geometric features of the blendees (e.g., curvature). It can be simply modified by controlling these blendee surfaces in ordinary surface designing. Second, less additional space and/or time is required. Instead of assigning large memory to store control meshes of the blended surface (in subdivision methods or trimmed B-spline methods), it is only necessary to generate and save N low-degree extended surfaces. Third, this model can blend all types of parametric surfaces defined in rectangular domains without any specified normal or derivative vectors. Fourth, it accepts incompatible and regressive input

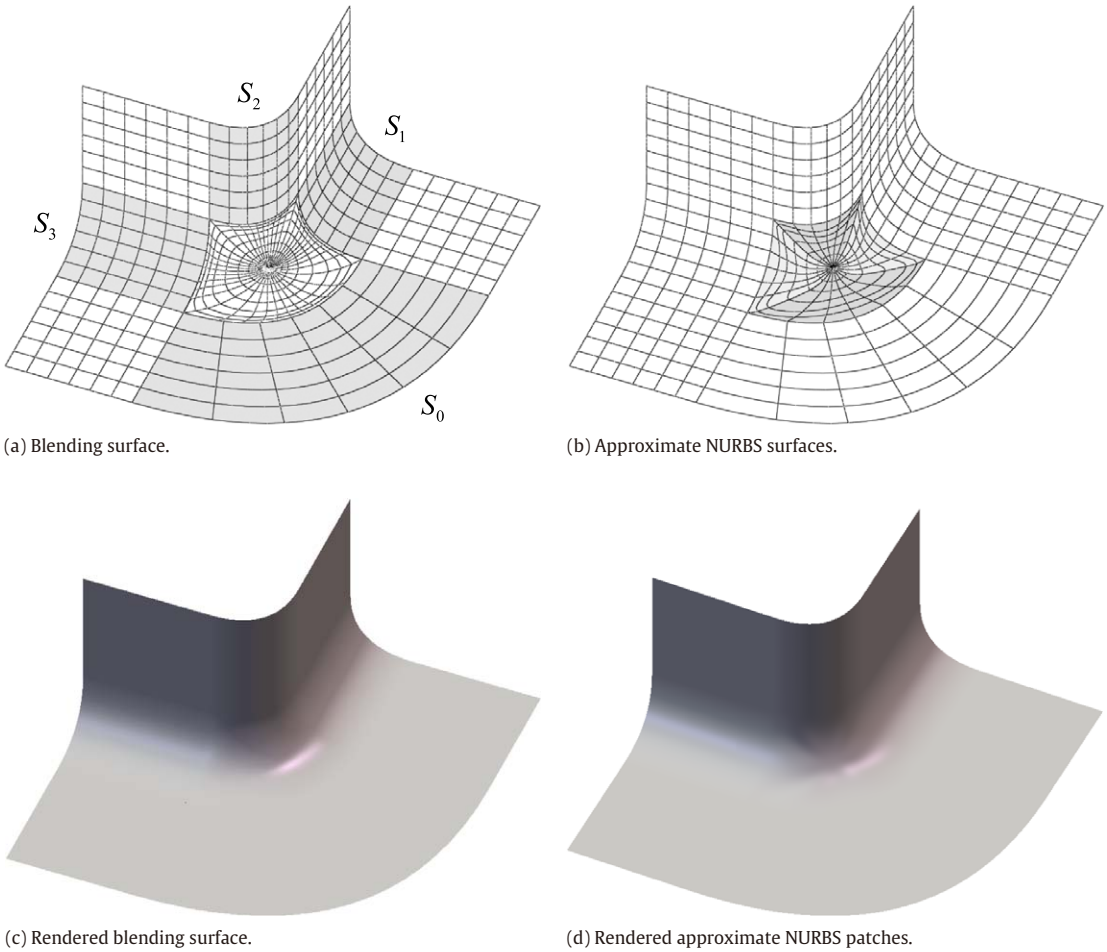

(a) Blending surface. (b) Approximate NURBS surfaces.

(c) Rendered blending surface. (d) Rendered approximate NURBS patches.

Fig. 13. Example 2: G^2 blending of a four-sided hole.

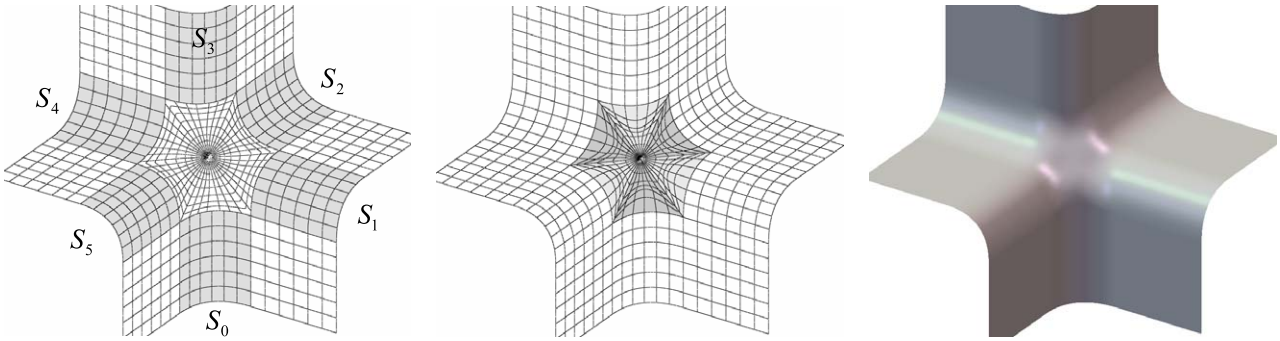

(a) Blending surface. (b) Approximate NURBS surfaces. (c) Rendered.

Fig. 14. Example 3: G^2 blending of a six-sided hole.

conditions. The examples in the following section show these advantages.

8. Examples

The multiple surface blending technique can be directly used in practical applications. The NURBS approximation method proposed in Section 6 extends its compatibility. In this section, we give several examples to demonstrate the results of different cases of vertex blending.

Example 1 shows a familiar instance in geometric modeling. Shown in Fig. 12, the edge blending technique generates a three-sided hole in the corner of the cube. We use two-degree Bézier surfaces in the edge blending. The hole is filled by a multiple blending surface with G^2 continuity. Fig. 12 (a) is the isoparametric mesh of the blending surface and its neighboring original surfaces. And Fig. 12 (c) is the rendered image of it. Fig. 12 (b) shows the approximate NURBS patches and Fig. 12 (d) is the rendered image of them. The degrees of the derivative curves are less than three because of the Bézier form of the original blendees. The second-order Taylor series expansion increases the degree of u-direction of the approximate surfaces (see Table 1). According to the steps of approximation discussed in Section 6, we get these three approximate NURBS patches.

Example 2 shows a more complicated instance. The edge blending generates four multiform surfaces. One of them is a flat

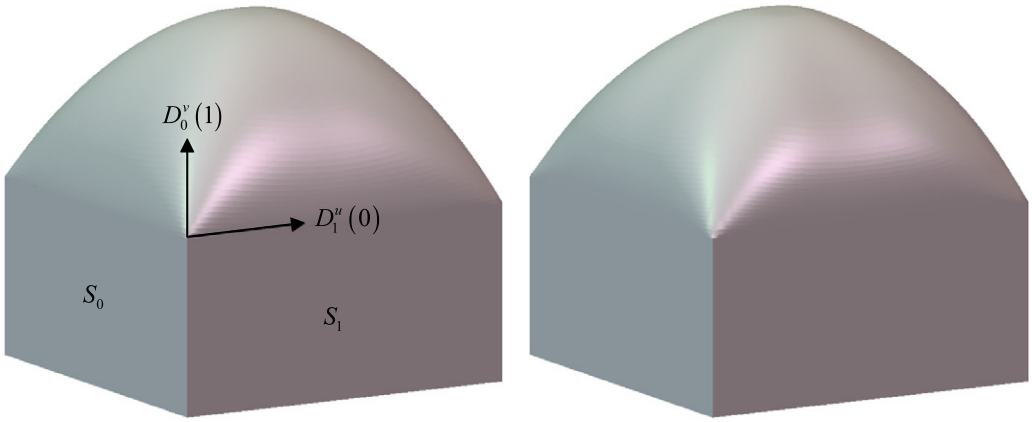

(a) G^1-contact blending. (b) G^2-contact blending.

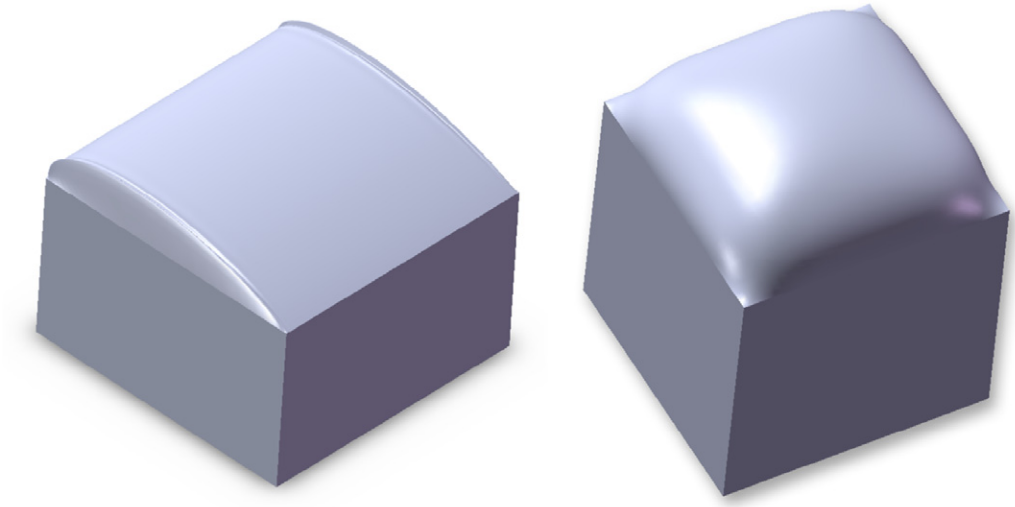

(c) G^1 filling result by SolidWorks 2007. (d) G^1 filling result by CATIA R18.

Fig. 15. Example 4: Blending incompatible surfaces.

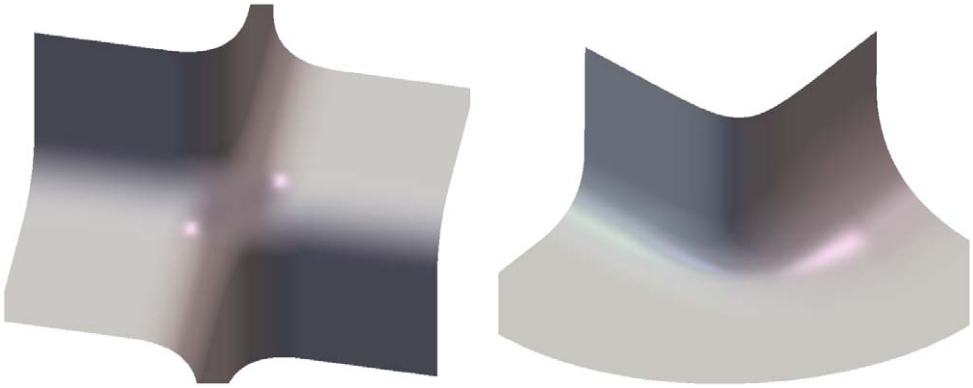

(a) G^3 blending of a six-sided hole. (b) G^3 blending of a four-sided hole.

Fig. 16. Example 5: G^3 blending.

rational Bézier surface. The others are all cylinder surfaces that can be represented in rational Bézier form. The degrees of the second-order derivative curves are three times the degrees of the original surfaces. The second-order Taylor series expansion increases the u-direction degree of the approximate patches (see Table 2). Only G^1 continuity is satisfied in the corner because of the cylinder form. Our method can still generate a smooth blending surface fulfilling G^2 continuity conditions everywhere except for the four corner points. Fig. 13 shows the results.

Example 3 presents the so-called three-convex–three-concave instance, which is a classical case in vertex blending. Six edges intersect at the center point. All of them are blended using the

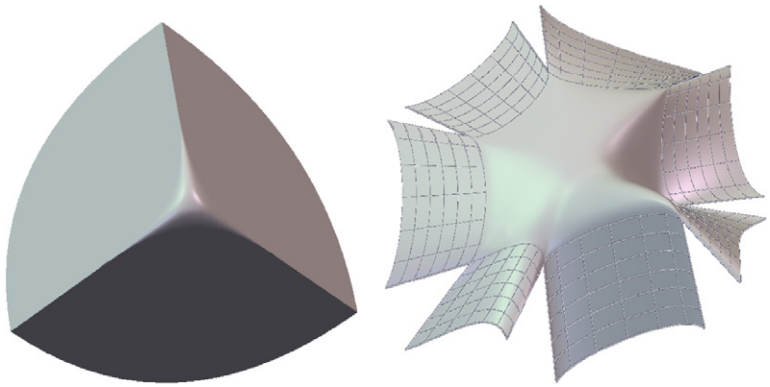

(a) G^3 blending of a three-sided hole with regressive corners.

(b) Blending irregular surfaces with incompatible boundaries.

Fig. 17. Example 6: Blending irregular surfaces.

Table 1
Surfaces in Example 1.

Original surfaces			Approximate surfaces of the blending surface		
Name	Type	Degree (u, v)	Name	Type	Degree (u, v)
S_0	Bézier	2, 1	N_0	Bézier	$2+2=4, 5$
S_1	Bézier	2, 1	N_1	Bézier	$2+2=4, 5$
S_2	Bézier	2, 1	N_2	Bézier	$2+2=4, 5$

Table 2
Surfaces in Example 2.

Original surfaces			Approximate surfaces of the blending surface		
Name	Type	Degree (u, v)	Name	Type	Degree (u, v)
S_0	Bézier	2, 1	N_0	NURBS	$2\times3+2=8, 5$
S_1	Cylinder	2, 1	N_1	NURBS	$2\times3+2=8, 5$
S_2	Cylinder	2, 1	N_2	NURBS	$2\times3+2=8, 5$
S_3	Cylinder	2, 1	N_3	NURBS	$2\times3+2=8, 5$

rolling-ball method. Then a six-sided hole is generated. It is filled by a blending surface, or N approximate NURBS patches (see Fig. 14).

Example 4 shows the result of blending four surfaces with totally incompatible boundaries. As discussed in Piegl's [13] paper, *the NURBS book* [25] and other books on differential geometry,

$$D_0^v(1) = \frac{\partial S_0}{\partial v}(u, v)\Big|_{\substack{u=1\\v=0}} = \frac{\partial S_1}{\partial u}(u, v)\Big|_{\substack{u=0\\v=0}} = D_1^u(0)$$

is the tangent compatibility condition (see the labels on Fig. 15). Generally, the two derivatives are not totally equal. At least they need to be parallel so that a scalar reparameterization can be applied to make them equal. In Fig. 15, the two derivatives are orthogonal instead of parallel. It is extremely difficult for Piegl's algorithm and other algorithms to solve that problem (see the results by SolidWorks and CATIA in Fig. 15 (c) and (d)). However, our multiple surface blending technique can still generate a logical and smooth surface fulfilling G^2-continuity conditions almost everywhere except the four points in the corner. The derivatives of the four corner points in the blending surface are set to the average of the two corresponding derivatives of the neighboring surfaces.

Example 5 shows two G^3 blending instances. Fig. 16 (a) is the G^3 blending result of a six-sided hole with cylindrical adjacent surfaces. Fig. 16 (b) is the generalization of Example 2. Three edges intersect at the center point. They are blended by the rolling-ball algorithm with different radii. Our multiple surface blending technique is used to fill the four-sided hole.

Example 6 shows two instances of blending irregular surfaces. Fig. 17 (a) is a G^2 blending result of three triangular NURBS surfaces. The blendees share three sharp corners where the two derivative vectors in the u-direction and the v-direction are superposed. They also share one regressive point, which is the corner of the original cube before blending. Fig. 17 (b) is a blending result of a seven-sided randomly generated hole with incompatible neighboring surfaces. It is more complicated than other regular models.

9. Conclusions

This paper proposes a model of blending N parametric surfaces with G^n continuity. Blendees are reparameterized into the form of polar coordinates and then blended simultaneously by a two-dimension basis function defined in the complex domain. Continuity conditions of the polar coordinate parametric surfaces and their NURBS-compatible form are also presented. The NURBS approximation algorithm extends its practicability. The model obtains G^n continuity and NURBS compatibility as well as having simpleness in construction and evaluation. It is directly used in filling N-sided holes without compatibility restrictions on the boundary.

Acknowledgements

The authors would like to thank Professors Chi C.-H., Liu Y.-S. and Zhang H., Doctors Yang Y. and Yang S. for their valuable suggestions, as well as the anonymous reviewers for their helpful comments. The research was supported by Chinese 973 Program (2010CB328001), the National Science Foundation of China (60625202, 90715043), and Chinese 863 Program (2007AA040401). The second author was supported by the Fok Ying Tung Education Foundation (111070). The last author was supported by ANR-NSFC (60911130368).

References

[1] Hartmann E. Parametric G^n blending of curves and surfaces. The Visual Computer 2001;17:1–13.
[2] Meek DS, Walton DJ. Blending two parametric curves. Computer-Aided Design 2009;41:423–31.
[3] Vida J, Martin RR, Várady T. A survey of blending methods that use parametric surfaces. Computer-Aided Design 1994;26:341–65.
[4] Choi BK, Ju SY. Constant-radius blending in surface modeling. Computer-Aided Design 1989;21:213–20.
[5] Lukács G. Differential geometry of G^1 variable radius rolling ball blend surfaces. Computer Aided Geometric Design 1998;15:585–613.
[6] Sun C, Zhao H. Generating fair, C^2 continuous splines by blending conics. Computer & Graphics 2008;33:173–80.

[7] Hartmann E. G^n-blending with rolling ball contact curves. In: Proceedings of the geometric modeling and processing. 2000. p. 385.
[8] Song QZ, Wang JZ. Generating G^n parametric blending surfaces based on partial reparameterization of base surfaces. Computer-Aided Design 2007;39:953–63.
[9] Hwang WC, Chuang JH. *n*-sided hole filling and vertex blending using subdivision surfaces. Journal of Information Science and Engineering 2003;19:857–79.
[10] Yang YJ, Yong JH, Zhang H, Paul JC, Sun JG. A rational extension of Piegl's method for filling *n*-sided holes. Computer-Aided Design 2006;38:1166–78.
[11] Gregory JA, Zhou JW. Filling polygonal holes with bicubic patches. Computer Aided Geometric Design 1994;11:391–410.
[12] Hahn J. Theory and practice of geometric modeling. Springer-Verlag; 1989.
[13] Piegl LA, Tiller W. Filling *n*-sided regions with NURBS patches. The Visual Computer 1999;15:77–89.
[14] Gregory JA, Lau VKH, Zhou JW. Smooth parametric surfaces and *N*-sided patches. In: Computation of Curves and Surfaces. 1989.
[15] Plowman D, Charrot P. A practical implementation of vertex blend surfaces using an *n*-sided patch. In: Proceedings of the 6th IMA conference on the mathematics of surfaces. 1994. p. 67–78.
[16] Hosaka M, Kimura F. None-four-sided patch expression with control points. Computer Aided Geometric Design 1984;1:75–86.
[17] Sabin MA. None-rectangular surface patches suitable for inclusion in a B-spline surface. In: Proceedings of enrographics. 1983. p. 57–69.
[18] Karčiauskas K, Peters J. Bicubic polar subdivision. ACM Transactions on Graphics 2007;26:14:1–6.
[19] Karčiauskas K, Myles A, Peters J. A C^2 polar jet subdivision. In: Proceedings of the fourth Eurographics symposium on geometry processing. 2006. p. 173–80.
[20] Karčiauskas K, Peters J. Bi-3 C^2 polar subdivision. ACM Transactions on Graphics 2009;28:48:1–12.
[21] Li GQ, Li H. Blending parametric patches with subdivision surfaces. Journal of Computer Science and Technology 2002;17:498–506.
[22] National Bureau of standards. Initial graphics exchange specification, version 3.0. 1986.
[23] Liang XZ, Che XJ, Li Q. G^2 continuity conditions for two adjacent B-spline surfaces. In: Proceedings of the geometric modeling and processing. 2004.
[24] Ye XZ. The Gaussian and mean curvature criteria for curvature continuity between surfaces. Computer Aided Geometric Design 1996;13:549–67.
[25] Piegl LA, Tiller W. The NURBS book. 2nd ed. Springer; 1997.
[26] Piegl LA, Tiller W. Symbolic operators for NURBS. Computer-Aided Design 1997;29:261–8.